Journal of Industrial Microbiology and Biotechnology, 2021, 48, kuab041

https://doi.org/10.1093/jimb/kuab041
Advance access publication date: 1 July 2021
Genetics and Molecular Biology of Industrial Organisms – Original Paper

Directed evolution of alditol oxidase for the production of optically pure D-glycerate from glycerol in the engineered *Escherichia coli*

Chao Zhang[1,2,‡], Qian Chen[1,‡], Feiyu Fan[1], Jinlei Tang[1], Tao Zhan[1,†], Honglei Wang[2,†], Xueli Zhang[1]

[1]Key Laboratory of Systems Microbial Biotechnology, Tianjin Institute of Industrial Biotechnology, Chinese Academy of Sciences, 32 Xiqidao, Tianjin Airport Economic Park, Tianjin 300308, China
[2]College of Chemistry and Life Science, Changchun University of Technology, Jilin, Changchun 130012, China
Correspondence should be addressed to: Tao Zhan. Tel: +86-22-84861946. E-mail: zhan_t@tib.cas.cn. Honglei Wang. Tel: +86-0431-85716473. E-mail: wanghonglei@ccut.edu.cn
[†]Present Addresses: 32 XiQiDao, Tianjin Airport Economic Park, Tianjin, 300308, China.
[‡]Chao Zhang and Qian Chen contributed equally to this work.

Abstract: D-glycerate is an attractive chemical for a wide variety of pharmaceutical, cosmetic, biodegradable polymers, and other applications. Now several studies have been reported about the synthesis of glycerate by different biotechnological and chemical routes from glycerol or other feedstock. Here, we present the construction of an *Escherichia coli* engineered strain to produce optically pure D-glycerate by oxidizing glycerol with an evolved variant of alditol oxidase (AldO) from *Streptomyces coelicolor*. This is achieved by starting from a previously reported variant mAldO and employing three rounds of directed evolution, as well as the combination of growth-coupled high throughput selection with colorimetric screening. The variant eAldO3-24 displays a higher substrate affinity toward glycerol with 5.23-fold than the wild-type AldO, and a 1.85-fold increase of catalytic efficiency (k_{cat}/K_M). Then we introduced an isopropyl-β-D-thiogalactopyranoside (IPTG)-inducible T7 expression system in *E. coli* to overexpress the variant eAldO3-24, and deleted glucosylglycerate phosphorylase encoding gene *ycjM* to block the consumption of D-glycerate. Finally, the resulting strain TZ-170 produced 30.1 g/l D-glycerate at 70 h with a yield of 0.376 mol/mol in 5-l fed-batch fermentation.

Keywords: Directed evolution, Alditol oxidase, D-glycerate, Glycerol, *Escherichia coli*

Introduction

As a potential multifunctional organic acid, DL-glycerate (2,3-dihydroxypropanoic acid, DL-glyceric acid [DLGA]) is one of the promising glycerol derivatives, which possess a wide variety of application areas, ranging from the synthesis of GA-based biodegradable branched-type polymers (Chiellini et al., 1990), acting as bioactive components of glyceric acid (GA) esters with antitrypsin activity from *Penicillium funiculosum* (Lešová et al., 2001), accelerating the oxidation of ethanol and acetaldehyde to detoxify in rats (Eriksson et al., 2007) and developing GA derivatives such as green surfactants acyl GAs (Tokuma et al., 2012), to the application of glucosylglycerate-derived compatible solutes through single-step enzymatic catalysis by sucrose phosphorylase (Sato et al., 2014; Sawangwan et al., 2009). Moreover, D-glycerate was also seen as a precursor and involved in various artificial enzyme-catalyzed synthesis routes for the synthesis of valuable products, including in the biotransformation of glycerol and glucose into value-added chemicals such as L-serine, L-alanine with two *in vitro* synthetic enzymatic cascades (Gmelch et al., 2019; Li et al., 2018). At present, D-glycerate is an attractive feedstock for a wide variety of pharmaceutical, cosmetic, and other industrial applications; thus, it is worth exploring to develop a commercially available method for converting crude glycerol into optically pure D-glycerate.

To summarize, several synthetic routes have been previously reported for the production of glycerate (Fig. 1; Table 1). The earliest reported the enzymatic production of D-glycerate from the decarboxylation of L-tartrate substrate via L-tartrate decarboxylase from *Pseudomonas* sp., with a molar yield of nearly 100% (Furuyoshi et al., 1989; Furuyoshi et al., 1991). Afterwards, most of the studies are motivated by the exploitation and utilization of crude glycerol, which is a major by-product of biodiesel industry, to produce value-added chemicals (Chen & Liu, 2016). Some studies have described application of the liquid-phase oxidation of glycerol with oxygen for the production of DL-glycerate by using precious metal catalyst (such as Au, Pd, Pt) (Demirel et al., 2007; Porta & Prati, 2004), while these routes also had some major disadvantages of catalyst cost, pollution control, and obtained a racemic mixture of DL-glycerate.

In contrast, the choice of biotechnologically produced glycerate from glycerol is a more sustainable alternative to traditional chemical oxidation for achieving commercial-scale production by microbial fermentation processes. For example, acetic acid bacteria (AAB) are obligate aerobic bacteria that have the ability to oxidize various sugars, sugar alcohols, and sugar acids for producing several valuable products by membrane-bound dehydrogenases, which is termed oxidative fermentation (Saichana et al., 2015). Hence, on the production of glycerate, several previous works had been carried out by Habe et al. for screening AAB to produce glycerate using crude glycerol as substrate under aerobic conditions (Habe et al., 2009a, 2009b). Of note, Habe et al. investigated glycerate-producing strains from 162 AAB strains and optimized fermentation conditions; the final glycerate production reached

Received: April 25, 2021. **Accepted:** June 26, 2021.

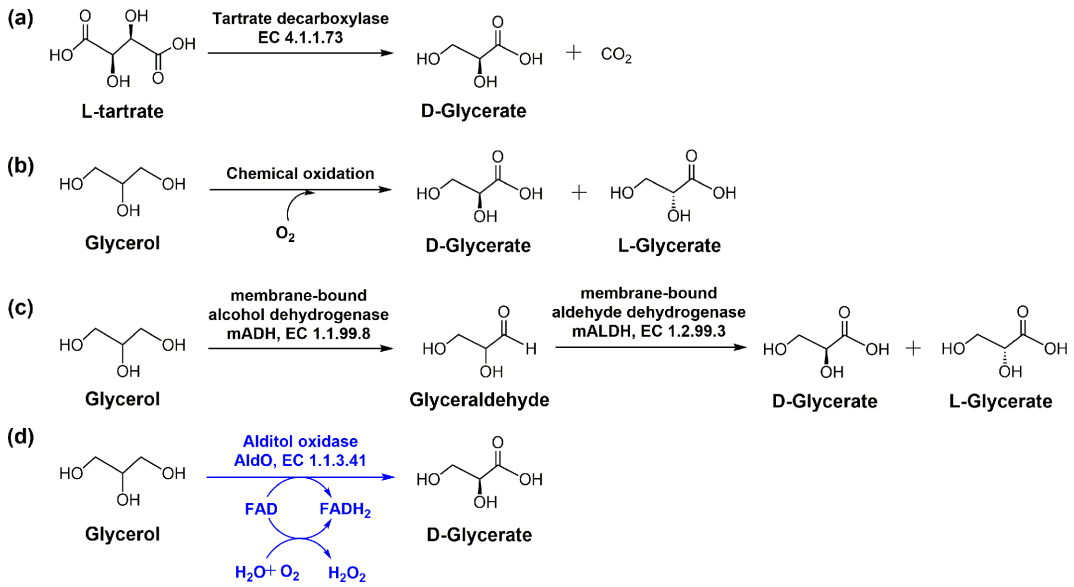

Fig. 1. Four routes for oxidation of glycerol to glycerate. (a) The decarboxylation of L-tartrate by L-tartrate decarboxylase from *Pseudomonas* sp.; (b) the chemical oxidation of glycerol to DL-glycerate by noble metal catalysts; (c) the microbial oxidation of glycerol to glycerate by acetic acid bacteria; and (d) the regioselective oxidation of glycerol to D-glycerate by AldO.

Table 1. Summary of Bio-Based DL-Glycerate Production on Several Substrates by Various Approaches

Substrate	Strain	Enzyme	Process	By-product	Optical purity	Titer (g/l)	Yield (mol/mol)	Productivity (g/l/h)	Ref.
L-tartrate	*Pseudomonas* sp. group Ve-2	L-tartrate decarboxylase	Whole-cell biocatalyst	——	>92% *ee*	53	1.0	0.44	(Furuyoshi et al., 1989)
L-tartrate	*Pseudomonas* sp. group Ve-2	L-tartrate decarboxylase	Whole-cell biocatalyst	——	——	106	1.0	2.36	(Furuyoshi et al., 1991)
Glycerol	*Acetobacter tropicalis* NBRC16470	mADH[a], mALDH[b]	Batch fermentation	——	——	22.7	——	0.24	(Habe et al., 2009a)
Glycerol	*Gluconobacter* sp. NBRC3259	mADH, mALDH	Batch fermentation	DHA	88.4%	45.9	——	0.48	(Habe et al., 2009c)
Glycerol	*Gluconobacter frateurii* NBRC103465	mADH, mALDH	Fed-batch fermentation	DHA	72%	136.5	——	0.95	(Habe et al., 2009c)
	Acetobacter tropicalis NBRC16470	mADH, mALDH			99%	101.8	——	0.85	
Glycerol	*Gluconobacter frateurii* THD32 mutant (Δ*sldA*)	mADH, mALDH	Fed-batch fermentation	——	——	89.1	——	0.93	(Habe et al., 2010)
Glycerol	*Escherichia coli* TZ-170	AldO	Fed-batch fermentation	——	99%	30.1	0.376	0.43	This study

[a]Membrane-bound alcohol dehydrogenase.
[b]Membrane-bound aldehyde dehydrogenase.

136.5 g/l with a 72% enantiomeric excess (*ee*) of D-glycerate after 7-days incubation by *Gluconobacter frateurii* NBRC103465 and produced 101.8 g/l of D-glycerate with a 99% *ee* by *Acetobacter tropicalis* NBRC16470 after 6-days incubation. They also first demonstrated that the pyrroloquinoline quinone-dependent membrane-bound alcohol dehydrogenase (PQQ-mADH) is responsible for catalyzing the oxidation of glycerol (Habe et al., 2009c). Further research suggested that the PQQ-mADH was encoded by *adhA* gene and catalyzing the oxidation of glycerol to glyceraldehyde in AAB, then the glyceraldehyde was sequentially oxidized to glycerate by the PQQ-mALDH (Habe et al., 2010; Habe et al., 2009c; Peters et al., 2013). Here lies an unanswered question—what mechanism determines the enantiomeric composition of the GA is still unknown (Habe et al., 2010), although PQQ-mADH derived from *Acetobacter tropicalis* NBRC16470 can more efficiently oxidize glycerol to the D-isomer, D-glyceraldehyde, which is then oxidized to D-glycerate (Habe et al., 2009c; Yakushi & Matsushita, 2010).

FAD-dependent alditol oxidase (AldO) is an alternative biocatalyst to produce D-glycerate, is first characterized from *Streptomyces coelicolor* A3(2) and displays promiscuous activities for the oxidation of several polylols and sugars as substrate. This enzyme

Table 2. List of Strains and Plasmids Used in This Study

Strain	Genotype	Source
Escherichia coli ATCC8739	Wild-type	Lab collection
E. coli Trans1-T1	F$^-$ *φ*80 (*lacZ*) ΔM15 Δ*lacX74 hsdR*(r_k^-, m_k^+) Δ*recA1398 endA1 tonA*	TransGen Biotech
E. coli BL21(DE3)	F$^-$ *ompT hsdSB*(r_B^-,m_B^-)*gal dcm rne131(DE3)*	Thermofisher
E. coli DH5*α*	F$^-$ *φ*80*lacZ*ΔM15 Δ(*lacZYA-argF*) U169 *recA1 endA1 hsdR17* (r_k^-, m_k^+) *gal-phoA supE44λ*$^-$ *thi*$^-$*1 gyrA96 relA1*	Thermofisher
TZ-099	*E. coli* DH5*α*, *glpK*::*kan*^{R}, *gldA*::*cm*^{R}	This study
TZ-108	*E. coli* ATCC8739, Δ*glpK*, Δ*gldA*, Δ*glxK*, Δ*garK*, Δ*glcDE*, Δ*hyi*, Δ*glxR*, Δ*garR*	(Zhan et al., 2020)
TZ-168	TZ-108, *rhaBAD*::P_{lacUV5}-T7RNAP, *ldhA*::P_{T7}-eAldO3-24	This study
TZ-170	TZ-168, Δ*ycjM*	This study
Plasmid	**Description**	**Source**
pET-30a(+)	Kan^R, pBR322 replicon, T7 promoter, T7 terminator	Novagen
pKD46	Amp^R, temperature conditional pSC101 replicon, P_{BAD} promoter, λRed recombinase	(Datsenko & Wanner, 2000)
pSC103-mAldO	Amp^R, mAldO (synthetic) from *Streptomyces coelicolor alditol* oxidase variant (V125M/A244T/V133M/G399R) under the control of an artificial promoter P_{M1-46}	This study
pET30a-mAldO	Kan^R, mAldO cloned into pET-30a(+) vector	This study
pET30a-eAldO2-15	Kan^R, eAldO1-48 cloned into pET-30a(+) vector	This study
pET30a-eAldO2-48	Kan^R, eAldO2-48 cloned into pET-30a(+) vector	This study
pET30a-eAldO3-24	Kan^R, eAldO3-24 cloned into pET-30a(+) vector	This study

belongs to the vanillyl-alcohol oxidase (VAO) family and performs selective oxidation of the terminal hydroxyl group of substrates to produce the corresponding sugars or *α*-hydroxy acids (Heuts et al., 2007; van Hellemond et al., 2009). Due to the by-product H_2O_2 during the oxidation process, AldO can also be used as a cleaning composition for cleaning and laundry applications (Kumar et al., 2013a). In contrast to AAB, AldO is highly regio- and enantioselective for the oxidation of C1-OH bond of glycerol substrate, and generates D-glycerate rather than D-glyceraldehyde as the final product. To improve the catalytic activity toward glycerol, an evolved variant mAldO (V125M/A244T/V133M/G399R) was screened from mutant libraries constructed through error-prone PCR and site-saturation mutagenesis, which exhibited a 2.4-fold increase in specific activity toward glycerol substrate than the wild-type AldO. Gerstenbruch et al. also confirmed the biotransformation of glycerol to D-glycerate by the whole cells which overexpressed AldO resulted in 2.0 g/l D-glycerate for a conversion of 6.3% with 99.6 % *ee* in 60 h (Gerstenbruch et al., 2012). This report offers a potential approach for the production of optically pure D-glycerate from glycerol by introducing protein engineering integrated with metabolic engineering in *Escherichia coli*.

The development of a highly efficient biotransformation strategy to produce optically pure D-glycerate from crude glycerol can be further optimized. In this study, inspired by Gerstenbruch et al.'s works (Gerstenbruch et al., 2012), we evolved mAldO toward glycerol substrate for three rounds of directed evolution, and constructed an isopropyl-*β*-D-thiogalactopyranoside (IPTG)-inducible T7 expression system in *E. coli* to overexpress the variant eAldO3-24 for the production of optically pure D-glycerate from glycerol.

Materials and Methods

Strains, Plasmids, Media, and Materials

All strains and plasmids used in this study are described in Table 2, and oligonucleotides are listed in Supplementary Table S1. *E. coli* Trans1-T1 strain was used as the cloning host (TransGen Biotech, Beijing, CN). *E. coli* BL21(DE3) was used for recombinant protein expression (Thermo Fisher Scientific, CN). *E. coli* DH5*α* strain was engineered to block both two native glycerol metabolic pathways, which generated a strain termed TZ-099 and was employed as the host for constructing mutant libraries of AldO. Bacteriophage T7 was utilized to lyse cells in 96 deep-well plates (Zhan et al., 2013). Based on our previously reported study (Zhan et al., 2020), *E. coli* strain TZ-108 was used as the parent strain for engineering to produce D-glycerate. The coding sequence of mAldO was synthesized with codon optimized for *E. coli* (GeneScript, Suzhou, CN) (Zhan et al., 2020).

For genetic manipulation, gene cloning, and protein expression, all strains were cultivated in Luria-Bertani (LB) medium containing 10 g/l NaCl, 10 g/l tryptone, and 5 g/l yeast extract. Antibiotics were added at the working concentrations: ampicillin (100 *μ*g/ml), chloramphenicol (34 *μ*g/ml), and kanamycin (50 *μ*g/ml). The following concentrations of inducers were used in this study: 2% arabinose and 0.1 mM IPTG. For high-performance liquid chromatography (HPLC) analysis and enzymatic activity assay, related standard substances and substrates were purchased from Sigma-Aldrich (St. Louis, USA).

Construction of Strains and Plasmids

Gene deletions and integrations were performed using λRed-mediated recombination (Datsenko & Wanner, 2000). The sequence of T7 RNA polymerase (T7RNAP) was amplified from *E. coli* BL21 (DE3) and used for chromosome integration. The plasmids pET30-serial were constructed by the method of circular polymerase extension cloning (CPEC) (Quan & Tian, 2011). These primers used for two-step homologous recombination and plasmid construction are listed in Supplementary Table S1.

Construction of AldO Mutant Libraries

In this work, error-prone PCR was employed to construct the first round mutant library. The plasmid pSC103-mAldO was constructed with a variant mAldO, which was reported from Gerstenbruch and used as a template for directed evolution (Gerstenbruch et al., 2012; Zhan et al., 2020). For error-prone PCR,

the amplification mixture (50 µl) contained ~5 ng template DNA, 1 µl EasyTaq® DNA Polymerase (5 units/µl, TransGen Biotech), 5 µl 10 × EasyTaq® buffer, 0.2 µM each primer (AldO-CF and AldO-CR, Supplementary Table S1), an unbalanced dNTP mixture of 0.2 mM each of dCTP and dTTP, 1.0 mM each of dGTP and dATP, and the increased Mg^{2+} concentration to 5 mM. The resulting PCR products were purified and cloned into pSC103 backbone under control of a strong constitutive promoter P_{lpp} via the CPEC method (Quan & Tian, 2011).

For synthetic shuffling, the method was modified and performed by assembling and annealing synthetic oligonucleotides with DNA fragments (200–300 bp), to obtain a shuffled library as previously described (Ness et al., 2002). These DNA fragments were from several evolved variants in the first round of directed evolution. Other 10 genes of AldO from *Streptomyces* genus were chosen as templates for synthesis of oligonucleotide fragments in synthetic shuffling, and their corresponding GenBank IDs, multiple sequence alignment, and molecular phylogenetic analysis are demonstrated in Supplementary Figs. S1 and S2. The coding sequence of mAldO was codon optimized for *E. coli* and synthesized as described (Zhan et al., 2020). Positions of introduced diversity residues into the backbone for synthetic shuffling are shown in Supplementary Table S2. Each synthetic oligonucleotide was 40 bases in length, the sequences of the forward oligonucleotides were represented by F1 to F19, and the other complementary reverse oligonucleotides were labeled with R1 to R16. All primers were purchased from Sangon Biotech (Shanghai, China).

To construct the second and third round mutant libraries, the synthetic shuffling was performed and modified from a previously reported method (Ness et al., 2002). The sequence of mAldO was amplified with primers pSC103-YZ-F and pSC103-YZ-R (Supplementary Table S1), and then the purified PCR products (150 ng/μl, 700 μl) were fragmented by ultrasonic treatment to generate 200–300 bp size DNA fragments as backbone in the assembling process; then these fragments were purified with high resolution agarose gels (MetaPhor®, Lonza) by using the QIAquick gel purification kit (Qiagen). Synthetic or fragmentation-based assembly reactions were carried out by primerless PCR. In a 50-µl mixture, all synthetic oligonucleotides were mixed with a final concentration of 0.2 μM, combined 300–500 ng DNA fragments, 0.8 mM dNTPs, 2.5 units of Taq polymerase. The following PCR program parameters were set: 1 cycle of 5 min at 94°C, 30 cycles of 30 sec at 94°C, 30 sec 40°C, 20 sec + 1 sec per cycle at 72°C, and 10 min at 72°C. Full-length chimeric sequences were obtained with flanking primers AldO-CF and AldO-CR (Supplementary Tables S1) in a standard PCR with 2 µl of primerless PCR products per 100 µl reaction as template, and the PCR program entailed 94°C for 5 min, 30 cycles of 94°C for 30 s, 60°C for 30 s, 72°C for 1.5 min, and 72°C for 10 min. The shuffled PCR products were purified with high-resolution agarose gels (MetaPhor®, Lonza), and mutant libraries were cloned by the method of CPEC into pSC103 vector (Quan & Tian, 2011) and transformed into *E. coli* TZ-099 host for the growth-coupled selection and subsequent screening for oxidase activity.

High-Throughput Screening of AldO Libraries

The high-throughput selection and screening system was performed in three steps consisting of growth-coupled selection, horseradish peroxidase-2,2'-azino-bis-(3-ethylbenzthiazoline-6-sulfonic acid) (HRP-ABTS) colorimetric assay, and shake flask rescreening. First, mutants were grown on M9 minimal medium using 20 g/l glycerol as sole carbon source at 37°C for 96 h. Following, these larger colonies were picked into 96-well deep-well plates (Thermo Scientific™ Nunc™ 2.0 ml) containing 0.5 ml LB medium plus 100 µg/ml ampicillin. After grown at 37°C and 800 rpm for 18 h, a stock solution of the bacteriophage T7 (100 μl) was added and cultured for 6 h to lyse cells as described previously (Zhan et al., 2013). A 160 μl of cell-lysis supernatant was transferred to a 96-well microtiter plate and mixed with 40 μl of reaction buffer, which contained 5 unit/ml HRP in 50 mM Tris-HCl buffer at pH 7.5, 2 mg/ml ABTS as an indicator (Sun & Yagasaki, 2003), and 50–100 mM glycerol as a substrate to screen AldO variants' activity. The reactions were proceeded at room temperature for 1 h and the absorbance change at 410 nm was measured and compared with the control plasmid (harboring a starting gene of mAldO) on an Infinite® 200 PRO Microplate Reader (Tecan, Switzerland).

Protein Expression and Purification

The purification of recombinant proteins was performed by gravity-flow chromatography with precharged Ni Sepharose™ (GE Healthcare). The coding sequences of mAldO and variants were cloned into the expression vector pET-30a(+) by employing CPEC method, and the resulting recombinant plasmids were electroporated into *E. coli* BL21(DE3). *E. coli* BL21 (DE3) cells were grown in LB medium containing 50 mg/l kanamycin, and recombinant protein expressions were induced by adding 0.1 mM IPTG when the cells reached 0.6–0.8 of OD600nm and cultured at 25°C for 18 h. Cells were harvested and resuspended in 50 mM Tris-HCl buffer (pH 7.5), then disrupted by sonication on ice and supernatants of the cell lysate collected by centrifugation (14 972 *g*, 30 min, 4°C) (Sigma 3–18 K). The supernatant was filtered through a 0.22 μm filter and loaded onto a pre-equilibrated HisTrap HP column (GE Healthcare). The recombinant protein was eluted with 200 mM imidazole in 20 mM sodium phosphate (pH 7.5) with 0.5 M NaCl. Further protein purification and concentration was obtained by Amicon® Ultra-15 10 K Centrifugal Filters (MERCK) with 50 mM Tris-HCl (pH 7.5). The purified protein was verified by a 10% SDS-PAGE gel.

Enzymatic Assay and Kinetic Parameter Determination

The activity of AldO was evaluated by measuring the rate of H_2O_2 generation from the oxidation of glycerol substrate under the HRP-ABTS coupled assay, as outlined previously (Arnold & Georgiou, 2003). The kinetic parameters for AldO variants were determined by varying the concentration of glycerol substrate. The reaction mixture (200 μl) containing 130 μl 50 mM Tris-HCl (pH 7.5), 20 μl 20 mg/ml ABTS, 20 μl 50 U/ml HRP, and 20 μl glycerol (20-800 mM) was incubated at 25°C for 5 min. The H_2O_2 products can be monitored by measuring the absorbance increase at 410 nm using the Infinite® 200 PRO Microplate Reader (Tecan, Switzerland). The kinetic constants K_m and k_{cat} were calculated by the Lineweaver-Burk plot in GraphPad Prism 8 software. Protein concentrations were determined by Bradford Protein Assay Kit using bovine serum albumin as a standard (Sangon Biotech, Shanghai, China). One unit (U) was defined as the amount of AldO generating 1 μmol H_2O_2 per minute under the assay conditions.

Multiple Sequence Alignment, Phylogenetic Tree Analysis and Molecular Modeling

Multiple sequence alignments were generated using ClustalW program and ESPript 3.0 web server (Larkin et al., 2007; Robert & Gouet, 2014). Based on the crystal structure of wild-type AldO

in its native oxidized state (PDB ID: 2VFV) (Forneris et al., 2008), the initial three-dimensional structures of AldO variant was modelled using the I-TASSER server (https://zhanglab.ccmb.med.umich.edu/I-TASSER/) (Roy et al., 2010). The secondary structure of prediction output was validated by PSIPRED program (Buchan & Jones, 2019), and the COACH program was used for prothetic group prediction (Yang et al., 2013). For further model refinement, the top scoring model created by I-TASSER was submitted to the GalaxyRefine program (http://galaxy.seoklab.org/index.html) for rebuilding and repacking side chain, subsequently suffered an overall structure relaxation by molecular dynamics simulation (Heo et al., 2013). The structure was visualized and manipulated using UCSF Chimera (v1.13.1) (Pettersen et al., 2004). Residue solvent accessibility surface (SAS) was calculated using Discovery Studio Visualizer software (Discovery Studio 2016, Accelrys Inc., San Diego, CA, USA), with parameters set as follows: probe radius was set at 1.40 Å by default, SAS values greater than 25% for exposed residues, and less than 10% for buried residues. The substrate glycerol was docked into the homology model of eAldO3-24 using the molecular docking program AutoDock Vina 1.1.0 (Trott & Olson, 2010).

D-glycerate Production in Shake Flasks and Bioreactor

To rescreen these improved variants, all candidate variant plasmids were transformed into the chassis strain *E. coli* TZ-108 and tested for the performance of producing D-glycerate from glycerol, which were performed in shake flasks containing 50 ml LB medium with 50 g/l glycerol, ampicillin (100 μg/ml), and the medium was buffered at pH 7.5 with 0.1 M 3-morpholinepropanesulfonic acid (MOPS). All the cultures were grown at 37°C, 250 rpm for 72 h. For validating the production of D-glycerate in engineered strains, the experiment was conducted in shake flasks and performed as described above. IPTG was added at 0.1 mM to induce T7 RNAP expression when the OD600 reached at 0.8. After 72 h growth, cells were collected for measurement of D-glycerate production with HPLC.

Strain TZ-170 was used for production of D-glycerate through fed-batch fermentation. The seed cultivation was inoculated 1 ml overnight culture and grown in 500 ml shake flask containing 100 ml LB medium at 37°C on 250 rpm for 16 h. Then the seed culture were transferred to a 5-l bioreactor (Labfors 4; Infors Biotechnology Co. Ltd.) containing 2 l fermentation medium, whose composition is described above (Zhan et al., 2020). Overexpression of AldO was induced by 0.1 mM IPTG when cells were grown for 4 h. Stirring speed was set between 500 and 1000 rpm and automatically adjusted by dissolved oxygen (DO) concentration set at 20%. The fermentation temperature was maintained at 37°C, and the pH was kept at 7.5 by automatic addition of 3 M NaOH. The feed solution containing 80 g/l glucose and 20 g/l yeast extract. The air flow was kept at 10 l/min. The cell biomass reached the maximum at 22 h, then pumped the feed solution into the bioreactor containing 700 g/l glycerol at a rate of 0.5–0.8 ml/min for 8 h.

Analytical Methods

Cell growth was monitored by measuring the optical density at 600 nm (OD600) using a SP-723 spectrophotometer (Spectrum Shanghai, China). The concentrations of glycerol and D-glycerate were measured using an Agilent 1200 Infinity series (Aminex HPX-87H, 7.8 × 300 mm, Bio-Rad) equipped with a refractive index detector (RI-150 Thermo Spectra, USA). The mobile phase consisted of 5 mM H_2SO_4 at a flow rate of 0.5 ml/min and the temperature of the column was maintained at 35°C.

Results

Growth-Coupled Selection and Screening Process for AldO Mutant Libraries

Owing to its promiscuous activities toward several polyols, AldO is an industrially interesting enzyme and has some promising prospects for applying in cleaning compositions, food industry, and synthetic organic chemistry (Kumar et al., 2013a). Firstly, we developed a high-throughput growth-coupled selection method, which relies on a novel alternative route via glycerol oxidation pathway to generate D-glycerate; then D-glycerate was phosphorylated by glycerate 2-kinase 1/2 (GarK/GlxK) to form 2-phospho-D-glycerate and enters the glycolytic pathway with glycerol as the sole carbon source (Fig. 2) (Ornston & Ornston, 1969; Zelcbuch et al., 2015). Here, to achieve this selection process, the host strain TZ-099 was obtained, which was derived from strain *E. coli* DH5α and deficient in two native glycerol metabolic pathways by inactivating both genes *glpK* and *gldA*, was used as screening host strain.

In this study, genetic complementary screening is a labor-saving tool for purging inactive mutants from a large number of colonies. For instance, in the first round of evolution, most of mutants were inactivity or low-activity and failed to grow under the selection condition, while about 5%–10% of the total number of functional colonies were able to be grown for 96 h; then these mutants were inoculated into 96 deep-well plates. Accordingly, in the second and third round of evolution, the incubation time of strain TZ-099 was gradually reduced to 24–48 h in the glycerol-M9 medium. Followingly, by means of the bacteriophage T7 lysis-based method (Zhan et al., 2013), the cell lysate supernatants containing AldO variants were used for oxidase activity screening based on a chromogenic reaction with ABTS as substrate, and read the absorbance increase at 410 nm (Arnold & Georgiou, 2003). These mutants exhibiting a higher absorbance at 410 nm than control group were subjected to further analysis, and the most efficient variants were used as templates for the next round of evolution (Fig. 3).

Directed Evolution of mAldO

To improve the catalytic activity of AldO for glycerol oxidation, we constructed a series of AldO mutant libraries by using several directed evolution approaches of random mutagenesis, synthetic shuffling, and DNA shuffling; and the variant mAldO served as evolutionary starting point for the efficient conversion of crude glycerol to optically pure D-glycerate with > 99% *ee* based on the previous study (Gerstenbruch et al., 2012; Zhan et al., 2020). In the first round of directed evolution, we used the method of error-prone PCR to generate a random mutagenesis library which contained an average of 1 to 3 residue substitutions per mutant. The high-throughput growth-coupled selection was performed on M9 mineral medium with glycerol as sole carbon source, about 10 000 clones were picked and screened for the quantitative analysis of H_2O_2 formation; fifteen variants were chosen and showed a higher value of OD410nm than the wild-type mAldO in the presence of 300 mM glycerol substrate, and these mutant plasmids were transformed into chassis strain TZ-108 for comparison of D-glycerate production in shake flasks (Fig. 4). Among these variants, three variants of eAldO1-43, eAldO1-74, and eAldO1-86 showed an improvement with 1.1 g/l, 1.15 g/l, and 1.17 g/l compared to the starting enzyme mAldO of 1.02 g/l, respectively.

Subsequently, to further increase genetic diversity and AldO activity, the variants eAldO1-43, eAldO1-74, and eAldO1-86 were

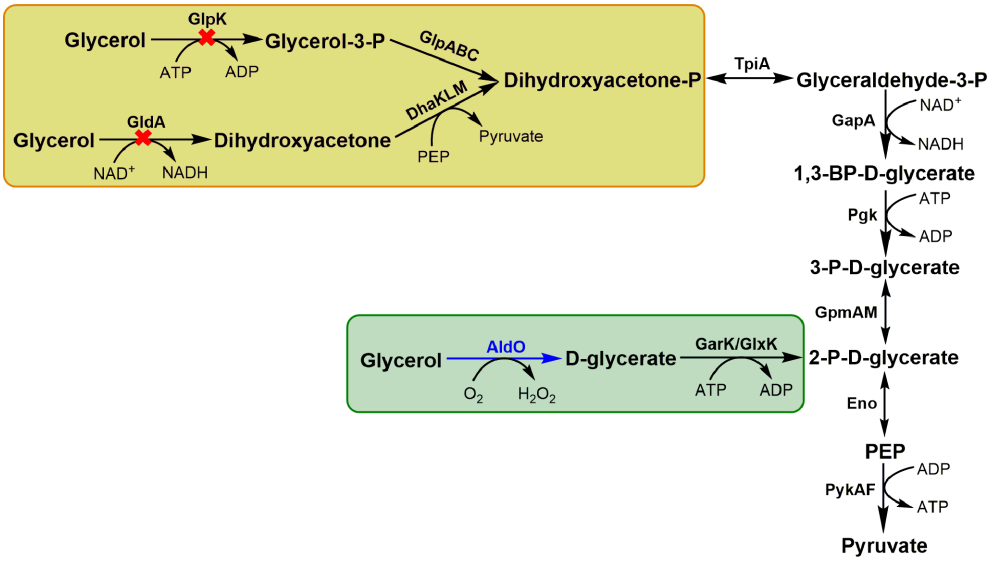

Fig. 2. Engineering of glycerol utilization pathways in screening host strain TZ-099. The exogenous pathway is represented in *blue* and the knocked-out genes are indicated by *red cross*. GlpK, glycerol kinase; GlpABC, glycerol-3-phosphate dehydrogenase; GldA, glycerol dehydrogenase; DhaKLM, dihydroxyacetone kinase; TpiA, triosephosphate isomerase; GapA, glyceraldehyde-3-phosphate dehydrogenase; Pgk, phosphoglycerate kinase; GpmAM, phosphoglycerate mutase; Eno, enolase; PykAF, pyruvate kinase; AldO, alditol oxidase from *Streptomyces coelicolor* A3(2); GarK/GlxK, glycerate 2-kinase 1/2.

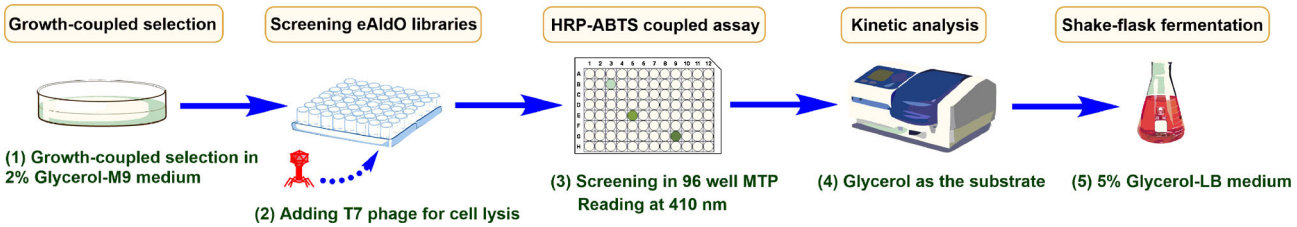

Fig. 3. Workflow of growth-coupled selection and enzyme activity screening process of mutant libraries for AldO. (1) High throughput assay used in the growth-coupled selection for mutant libraries of AldO expressed in strain TZ-099 with glycerol-M9 medium. (2) Larger colonies were picked into 96 deep-well plates and cultured with LB medium for overnight, T7 bacteriophage was then added to lysis cells and cultured for 6 h, and further centrifuged to release AldO variants' protein in supernatants. (3) HRP-ABTS (horseradish peroxidase and 2,2'-azino-bis-(3-ethylbenzthiazoline-6-sulfonic acid)) oxidation assay used in the screening of AldO variants in 96-well microtiter plate (MTP), and measured absorbance values at 410 nm by using Microplate Reader. (4) Comparison of the screened variant activities on glycerol substrate and the enzymatic kinetic parameters of final variants were determined. (5) Production of D-glycerate from evolved AldO variants expression on chassis strain TZ-108 in shake flask with 5% Glycerol–LB medium.

selected as backbone for the second round of evolution by using a modified method of synthetic shuffling, and eAldO1-86 was used as the control group in the 96-well plate screening. For the synthetic shuffled library, 11 *AldO* genes from *Streptomyces* sp were selected as templates to expend the natural sequence diversity in the recombination processes. The multiple sequence alignment and molecular phylogenetic analysis of AldOs are depicted in Supplementary Figs. S1 and S2. The 34 mutation sites were distributed throughout the sequence and these oligonucleotide fragments containing replace residues are listed in Supplementary Table S2 accordingly. After the growth-coupled selection of enrichment process as above, about 8000 clones were isolated from the shuffled library and screened with HRP-ABTS oxidation assay, and 200 mM glycerol was used as substrate for high-throughput screening. Two variants eAldO 2–11 and eAldO2-13 exhibited a higher activity on glycerol substrate than the control group of eAldO1-86. Correspondingly, the expression of mutants eAldO2-11 and eAldO2-13 showed 32%–49% increase compared with wild-type mAldO for the production of D-glycerate (Fig. 4).

Furthermore, based on the second round of efficient AldO variants, we combined these beneficial mutations and continued the introduction of more residue modifications by the synthetic shuffling for the third round of directed evolution. Then, the proportion of functional clones was significantly higher than the first round of evolution and increased from 5%–10% to 20%–30%, and grew faster than the original library with decrease in incubation time from 96 h to 48 h. Finally, about 15 000 active clones were picked and screened for oxidase activity using glycerol substrate. The chassis strain TZ-108 expressing these more efficient variants were able to produce 1.85 g/l, 1.94 g/l, and 2.53 g/l D-glycerate, respectively. Finally, after two rounds of shuffling eAldO mutants in the presence of several synthetic oligonucleotides harboring a cluster of nonconserved residues (Supplementary Table S2), the libraries exhibited more genetic diversity than the first round and the isolated active variants containing 11–14 mutations with a highly enriched in several sites (Fig. 4a). By contrast, the harboring variant eAldO3-24 of low copy number recombinant plasmid improved the yield of D-glycerate by 2.48-fold higher than the mAldO.

(a)

Enzyme	Mutations
eAldO1-43	R22C
eAldO1-74	M182I, V365A
eAldO1-86	A75V, F262L
eAldO2-11	R22C, D27A, D56A, S68P, V112I, V148T, A351R
eAldO2-13	R22C, D27A, D56A, A75T, F262L, E383R
eAldO3-23	R22C, D27A, S68G, A75V, M125V, S129P, V148I, R232Q, F262L, T318I, A368G, V379A, E383D
eAldO3-14	R22C, D27A, D56A, S68G, A75V, S129R, V148T, R232Q. F262L, E310D, T318I, A368G, V379A, E383G
eAldO3-24	R22C, D27A, S68P, A75V, S129P, V148T, R232Q, F262L, E310D, A368G, E383R

(b)

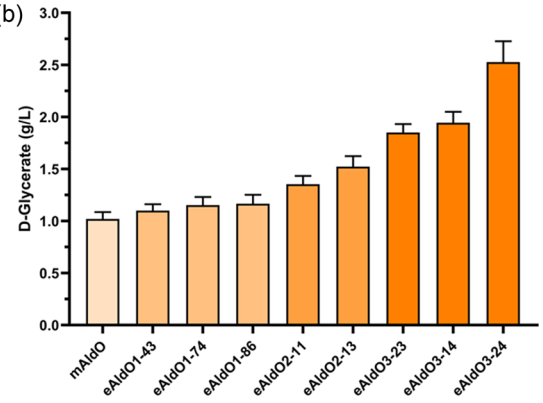

Fig. 4. Summary of mutations and comparison of D-glycerate production in mAldO and each evolved variant. (a) The list of modification of residues in each variant from three rounds directed evolution, which was based on the previously mutant mAldO (V125M/V133M/A244T/G399R). (b) D-glycerate production from variants and mAldO recombined plasmids were expressed in chassis strain TZ-108 for shake flask fermentation. Three independently cultured replicates were performed for each strain. The error bars represent the standard deviations.

Table 3. Kinetic Parameters of AldO Variants Along the Directed Evolution Process

Enzyme[a]	Specific activity (mU/mg)[c]	K_m (mM)	k_{cat} (s^{-1})	k_{cat}/K_m ($s^{-1}M^{-1}$)
Wild-type[b]	260 ± 25	350 ± 50	1.6 ± 0.1	4.6
mAldO	673.24 ± 14.85	109.7 ± 6.483	0.72 ± 0.16	6.56
eAldO2-11	877.16 ± 11.70	98.97 ± 3.84	0.70 ± 0.84	7.07
eAldO2-13	734.34 ± 2.61	81.57 ± 5.00	0.59 ± 0.16	7.23
eAldO3-24	834.08 ± 11.01	66.91 ± 3.12	0.57 ± 0.11	8.52

[a]Annotation of variants: The first letter e stands for evolved enzyme, the first digit relates to the number of evolutionary rounds, and the second digit represents a serial number assigned to each mutant in the rescreening process.
[b]The catalytic parameters were measured as described in van Hellemond et al., 2009.
[c]Enzymatic parameters were determined with purified recombinant protein with six His-tags at the C-terminal, and presented are mean ± s.d. values obtained from three independent experiments.

Kinetic Parameters and Molecular Modeling Analysis of AldO Variants

As the evolving of AldO improved the catalytic activity toward glycerol by the two-stage selection and screening process, the specific activity and catalytic efficiency (k_{cat}/K_m) of variants were gradually raised due to the iteration evolution. Kinetic parameters of all chosen mutants obtained in the screening process were determined using glycerol concentration varying in the range of 20–800 mM. Among them, the most active variant eAldO3-24 was isolated from the third-shuffled library and exhibited a 1.85-fold higher catalytic efficiency toward glycerol substrate (k_{cat}/K_m = 8.52 s^{-1} M^{-1}) than the wild-type AldO (k_{cat}/K_m = 4.6 s^{-1} M^{-1}) (van Hellemond et al., 2009), and 1.3-fold higher than the starting enzyme mAldO, whose kinetic parameters were determined in this study (Table 3) (Zhan et al., 2020). Encouragingly, the substrate specificity of the following evolved AldO variants toward glycerol were remarkably increased compared with the wild-type AldO—the K_m value of eAldO3-24 was prominently decreased by 5.23-fold from 350 ± 50 mM to 66.91 ± 3.12 mM, and also decreased by 1.64-fold comparable to mAldO. However, the turnover number (k_{cat}) of eAldO3-24 was calculated to be 0.57 ± 0.11 s^{-1} with 2.8-fold lower than the wild-type AldO, so that the k_{cat} values had no improvements in previous and our current studies.

To reveal the relationship between the structural change and catalytic activity of variant eAldO3-24, based on the crystal structure of wild-type AldO from *S. coelicolor* A3(2) (PDB code 2VFR) as a template (Forneris et al., 2008), the structural model of eAldO3-24 was generated by homology modelling using the I-TASSER online server (Roy et al., 2010), which possesses 96% sequence identity with the wild-type AldO. Though, this variant harboring 15 mutations were evenly distributed throughout the variant, and not located at substrate binding sites, molecular oxygen channel, and catalytic cavity (Fig. 5; Supplementary Fig. S3), the improved substrate affinity may be attributed to a subtle conformational change around the active site, and thus elevated enzymatic activity and selectivity toward glycerol. Furthermore, the solvent accessibility of protein residues is important for protein folding, solubility, and conformational stabilization. The solvent accessible surface of variant eAldO3-24 was analyzed on the structural model of eAldO3-24 by the Discovery Studio Visualizer, most of mutation sites are located at the surface of the protein, except for S129P, V133M, and A368G mutations were classified as buried residues, while V133M was introduced in previous study (Gerstenbruch et al., 2012). And the buried residues V125M and S129P were situated between α-helix 3 and disordered loop, which were located adjacent to V133M and belonged to a motion region in MD simulations (Gerstenbruch et al., 2012). Also, other 12 mutations were located on the surface of protein and perhaps involved in protein solubility and folding, which had positive effects on the total enzyme activity of AldO and the subsequent construction of D-glycerate producing strain. This suggests that the improvement of variants' catalytic efficiency was determined by a combinatorial effect of multiple mutations. Further structure solution will be needed to advance our understanding on how these changes affect the catalytic properties of the variant.

Construction of the D-Glycerate Producing Strain

To elevate the expression level of AldO and construct an optically pure D-glycerate producing strain from glycerol in this study, a 4.8 kb fragment, which include the repressor gene *lacI*, β-galactosidase gene (*lacZ*), and T7 RNA polymerase encoding gene under the control of the promoter *lac*UV5, was amplified from the strain *E. coli* BL21(DE3) and then integrated in the *rhaBAD* site of the glycolate producing chassis strain TZ-108 via λRed homologous recombination (Zhan et al., 2020). In this chassis strain, the genes including *glxK* and *garK* (encoding glycerate 2-kinase 1/2), *glxR* and *garR* (encoding tartronate semialdehyde reductase) were knocked-out, which involved the phosphorylation and reversible reactions of NAD^+-dependent oxidation of D-glycerate and played

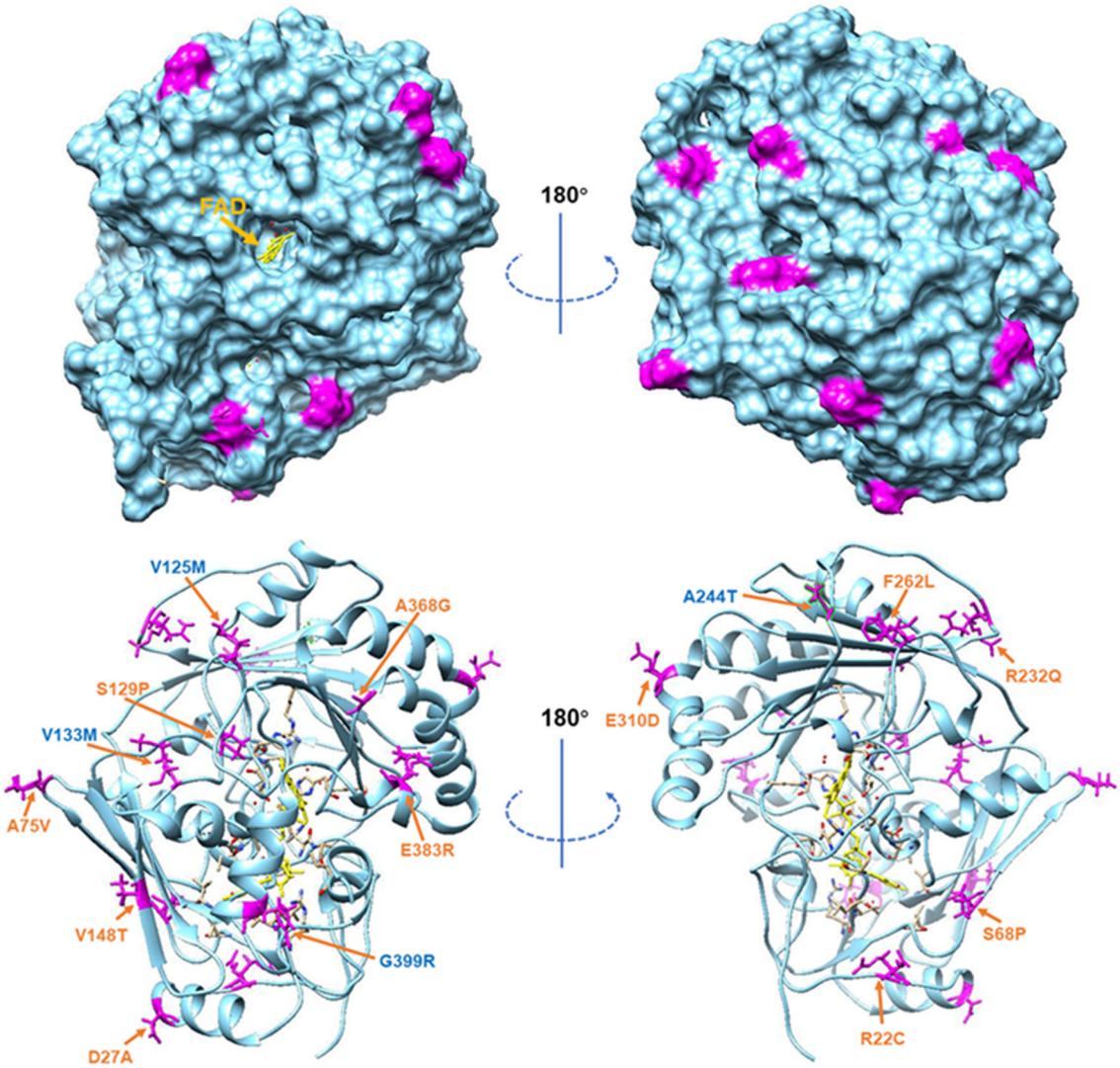

Fig. 5. Surface and ribbon diagram representation of the predicted structure of variant eAldO3-24. All mutated residues are shown as sticks and labeled. Residues were mutated in this study are labeled in yellow, and the residues derived from the starting gene mAldO are depicted in blue.

Table 4. The Production of D-Glycerate Using Engineered *Escherichia coli* Strains

Strain[a]	Genetic modification	D-glycerate (g/l)[b]	D-glycerate yield (mol/mol)	Glycerol consumption rate (g/l/h)	Cell mass (g/l)[c]
TZ-168	TZ-108, *rhaBAD*::P_{lacUV5}-T7RNAP, *ldhA*::P_{T7}-eAldO3-24	0.51 ± 0.02	0.23 ± 0.01	0.03 ± 0.002	0.80 ± 0.01
TZ-170	TZ-168, Δ*ycjM*	1.60 ± 0.03	0.20 ± 0.03	0.09 ± 0.004	2.84 ± 0.03

[a]Fermentations were carried out in shake flasks with LB medium containing 50 g/l glycerol. The medium was buffered at pH 7.5 with 0.1 M MOPS buffer. The inoculate initial OD600nm was 0.1, and 0.1 mM IPTG was added when cells grown to OD600nm of 0.5.
[b]Three repeats were performed and the error bars represent standard deviation.
[c]Cell mass was calculated by measuring the OD600nm (340 mg dry cell wt l^{-1} at 1.0 OD600) (Martinez et al., 2007).

roles in D-glucarate/D-galactarate/glycolate/glyoxylate degradation pathways (Cusa et al., 1999; Ornston & Ornston, 1969). Subsequently, the expression cassette of P_{T7}-eAldO3-24 was obtained from the plasmid pET30a-eAldO3-24 (Table 2) and inserted into *ldhA* site, resulting in initial strain TZ-168. So far, the one-step enzymatic catalysis pathway for producing D-glycerate from glycerol was constructed in *E. coli*. In shake flask fermentation, the initial strain TZ-168 produced 0.51 g/l in 72 h with molar yield of 0.23 mol/mol-glycerol (Table 4).

Besides, glucosylglycerate phosphorylase (encoded by *ycjM*), which was located in a cluster of the *ycj* genes in *E. coli*, catalyzed the synthesis of the compatible solute glucosylglycerate (α-[1,2]-D-glucose-D-glycerate) from α-D-glucose 1-phosphate and D-glycerate (Franceus et al., 2017; Mukherjee et al., 2018). Based on previous studies of Mukherjee, the K_m for D-glycerate was determined to be 4.4 mM in the presence of 10 mM α-D-glucose 1-phosphate, and with a k_{cat} = 295 s^{-1}, k_{cat}/K_m = 6.7 × 10^4 M^{-1} s^{-1} (Mukherjee et al., 2018). To further reduce D-glycerate

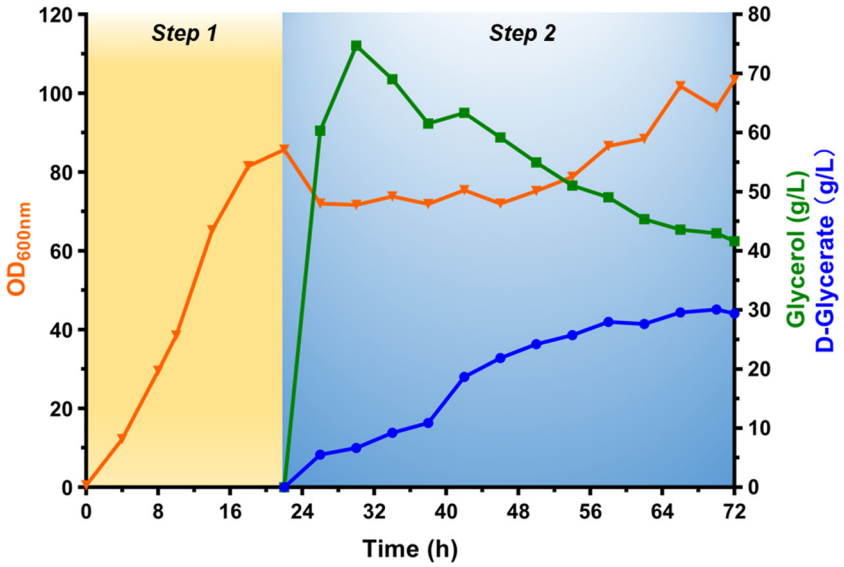

Fig. 6. Fed-batch fermentation for the production of D-glycerate from glycerol by the strain TZ-170. The orange line represents cell biomass (*triangles*), the green line represents glycerol (*squares*), and the blue line represents D-glycerate (*circles*).

consumption, next we deleted *ycjM* and resulting strain TZ-170, which produced 1.6 g/l D-glycerate and with 3.1-fold higher than that of the parent strain TZ-168, and showed an improvement of cell growth (1.25-fold) and glycerol consumption rate (3-fold), but there was no significant enhancement of D-glycerate yield (0.20 mol/mol *versus* 0.23 mol/mol) (Table 4), indicating that D-glycerate can readily enter the synthesis of glucosylglycerate to accumulate osmotic protective solutes inside the cell.

Production of D-glycerate by Fed-Batch Fermentation

The fed-batch fermentation for the production of D-glycerate was conducted using strain TZ-170 in a 5-l fermenter, and this process was carried out in complex medium with two steps (Fig. 6). To avoid H_2O_2 toxicity for the cell growth caused by the glycerol-oxidizing activity of AldO, glucose was used as the only carbon source for the fermentation step 1, and the eAldO3-24 was induced by the addition of 1 mM IPTG when cells were grown for 4 h. The glycerol feeding solution was pumped into the fermenter when cells were grown to the maximum OD of 85.7 from 22 h to 30 h, and 273.6 g glycerol supplement was fed in this process. As shown in Fig. 6, the addition of glycerol substrate triggered AldO catalytic reaction, and a large amount of by-product H_2O_2 was generated and inhibited cell growth from 24–56 h. Between 56 and 72 h, a gradually increasing trend of the OD600nm was observed. We speculate that there are two possibilities: One is that the water evaporation results in an increase of OD value of fermentation broth; another is that the cells exhibited a diauxic growth curve, which may be related to the intermediate product of glycerol oxidation catalyzed by AldO, glyceraldehyde fed into the central carbon metabolic pathway of *E. coli*. At the end of fermentation, the accumulation of D-glycerate reached up to 30.1 g/l at 70 h with a productivity of 0.63 g/h/l. Meanwhile, the glycerol to D-glycerate yield was 0.376 mol/mol, which is much lower than the theoretical yield (1 mol/mol).

Discussion

Previous studies have shown AldO acts as a flavin dependent oxidase primarily oxidizing alditols to D-aldoses, and involved carbohydrate degradation for sorbitol or xylitol metabolism (Heuts et al., 2007). Significantly, the characterization of promiscuous substrate specificity of AldO offers an attractive alternative for reacting with a broad range of substrates, which can serve as a versatile biocatalyst for the stereoselective oxidation of alditols and 1,2-diols to form the corresponding D-aldoses and α-hydroxy carboxylic acids (van Hellemond et al., 2009). However, due to the structural difference of substrate molecules in the active cavity (Forneris et al., 2008), the substrate preference of AldO toward C5 and C6 polyol substrates (xylitol, D-sorbitol, and D-mannitol) has a higher affinity than shorter polyols (glycerol, L-threitol), primary alcohols and diols (van Hellemond et al., 2009), which may be related to the structural difference of substrate molecules in the active cavity (Forneris et al., 2008). In addition, the substrate scope of a thermostable alditol oxidase (HotAldO) from *Acidothermus cellulolyticus* 11B was reported by Winter et al., which exhibited a highly similar substrate preference toward polyols as *S. coelicolor* AldO (Winter et al., 2012). In contrast, to enlarge the space of active cavity for accommodating glycerol as an efficient substrate, Nguyen et al. designed and mutated two key residues in the vicinity of the active site of alcohol oxidase from *Phanerochaete chrysosporium* (PcAOX, EC 1.1.3.13), which obtained a single point mutant F101S with significantly improved activity toward glycerol than the wild-type ($k_{cat} = 3\ s^{-1}$ *vs.* $k_{obs} = 0.2\ s^{-1}$) (Nguyen et al., 2018). Structurally, similar to other known flavoprotein oxidases, the size of the binding pocket that has an essential role in determining the substrate acceptance scopes and catalytic activity of AldO (Dijkman et al., 2013; Mattevi et al., 1997). Thus, the further improvement can be expected by reducing the size of the active-site cavity of AldO variant to enhance catalytic efficiency for the selective oxidation of these small molecular alcohols, which would offer a promising candidate biocatalyst for industrial applications or the development of oxidase-based biosensors.

In this study, we took advantage of the directed evolution methods of random mutagenesis and synthetic shuffling, combining with two steps of growth-coupled selection and ABTS-HRP colorimetric screening toward glycerol substrate, and obtained an evolved variant eAldO3-24 from three rounds of evolution with an improvement of 1.3-fold–higher catalytic efficiency than the starting enzyme mAldO. The variant eAldO3-24

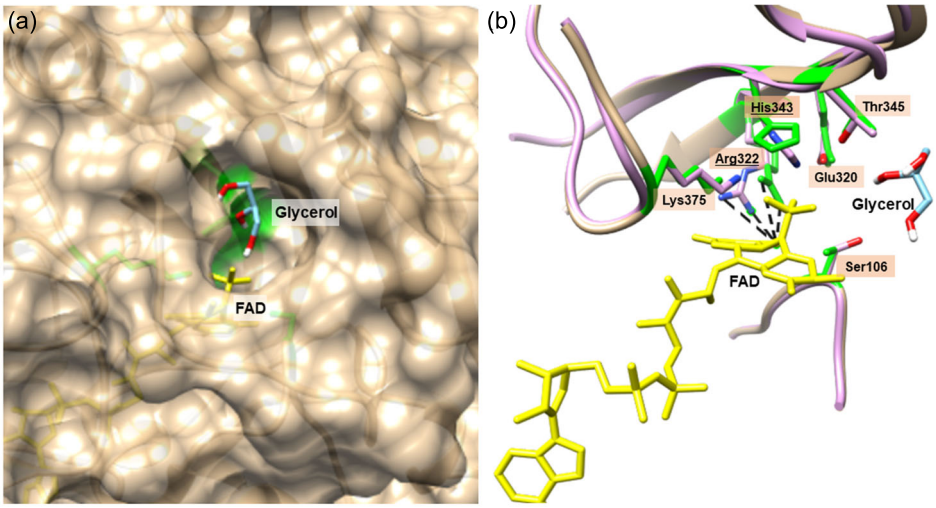

Fig. 7. Docking representation of glycerol substrate in the wild type AldO (PDB entry 2VFV) and variant eAldO3-24. (a) Close-up view of the surface around the catalytic pocket in variant eAldO3-24. The glycerol substrate (blue stick model) is accommodated in the active site cavity of the AldO, facing the isoalloxazine ring of the FAD cofactor (yellow stick model). (b) Superposition of docking poses of the glycerol ligand with the active site residues in the structures of wild type AldO (green) and eAldO3-24 (purple). Residues that involve in substrate binding and activation are labelled as stick model. Residues of Arg322 and His343 involved in conformational changes are underlined.

was integrated into the glycolate producing strain and under the control of T7 promoter and deleted gene *ycjM* encoding glucosylglycerate phosphorylase to block the conversion of D-glycerate to α-(1,2)-D-glucose-D-glycerate in the osmoprotectant biosynthesis pathway, an engineered strain *E. coli* TZ-170 was obtained, which achieved the bioconversion of glycerol to produce optically pure D-glycerate with a titer of 30.1 g/l at 70 h and the yield was 0.376 mol/mol.

To gain insights into the structure–activity relationship of the variant eAldO3-24, we used the 1.72 Å crystal structure of AldO from *Streptomyces coelicolor* A3(2) (PDB entry 2VFV) as a template for homology modeling of eAldO3-24 (sequence identity of 96%) (Forneris et al., 2008), and the ligand glycerol was docked into the AldO catalytic cavity as shown in Fig. 7. As previously reported, the position of glycerol binding is similar to the natural substrate xylitol in the docking model, which is facing the isoalloxazine ring of the FAD cofactor and interacted with hydroxyl groups with Ser106, Glu320, and Thr345 through hydrogen-bonding. In addition, most of the active site residues were highly overlaped in the superposition of two models. Yet there are slight conformational changes in the variant eAldO3-24: The guanidinium moiety of Arg322 and the imidazole ring of His343 (Fig. 7). Conserved residues Arg322 and Lys375, as shown in the Fig. 7b, are involved in the interaction with the substrate O1 atom through two hydrogen bonds between the guanidinium moiety of Arg322 and the amino group of Lys375. Especially, the residue His343 plays an important role in determining the size and shape of the substrate channel in catalytic cavity, and the C1-OH bond of glycerol substrate is bonded between the imidazole ring of His343 and the isoalloxazine ring of the FAD cofactor to form a sandwich structure (Forneris et al., 2008). Therefore, it is believed that the conformation changes of these two critical residues have a positive effect on the improvement of the substrate affinity of the variant eAldO3-24 toward glycerol. In addition, due to the cooperative interactions of multiple mutation sites in evolved mutants, it is commonly referred to as the epistatic effects, which is involved in substrate binding and catalytic cycle by affecting the secondary structures of protein and changing the enzyme conformational dynamics (Acevedo-Rocha et al., 2021). Further detailed studies will help us reveal potential roles of all mutation sites, including crystallographic data and enzymatic mechanism.

However, an obvious question here is why the obtained D-glycerate yield was far below the theoretical value? Similarly, the biotransformation of glycerol to D-glycerate by whole-cells with expressing AldO-His recombinant protein reached a conversion of 6.3% at 60 h (Gerstenbruch et al., 2012). One possible explanation is that glyceraldehyde is the intermediate product of AldO catalyzed glycerol oxidation, which was metabolized by other enzymes and entered the central carbon metabolic pathway of *E. coli*. In truth, Gerstenbruch et al. assumed that the glycerol oxidation catalyzed by AldO is a two-step reaction, and they also validated that the oxidase activity wild-type AldO was 185 mU/mg toward glyceraldehyde, which was equivalent to 71% of the enzyme activity for glycerol substrate (Gerstenbruch et al., 2012). Hence, we infer that the difference in substrate affinity and catalytic efficiencies of AldO toward glycerol and glyceraldehyde is responsible for the low yield of D-glycerate, and a detailed kinetic property of AldO active on C3 polyol and aldehyde substrates is required in the future.

Finally, this is the first study to achieve the production of optically pure D-glycerate in *E. coli* by fed-batch fermentation. Several different sources of AldOs have proven to be a potential biocatalyst for stereoselective oxidation of polyols in several biotechnological applications, our study provides an alternative way of producing optically pure D-glycerate by the AldO from *S. coelicolor* and the construction of a novel glycerol oxidation route in the screening host strain TZ-099, which can serve as a supplement for improving glycerol utilization in *E. coli* and other species. In addition, our study shows that the growth-coupled selection strategy can be employed to pre-evaluate a large number of mutants from each round library, this high-throughput selection protocol is also suited for the evolution of other key enzymes in some metabolic pathways.

Supplementary Material

Supplementary material is available online at *JIMB* (*www.academic.oup.com/jimb*).

Funding

This work was supported by grants from National Key R&D Program of China (2019YFA0904900).

Conflict of Interest

There is no conflict of interest associated with this study.

References

Acevedo-Rocha, C. G., Li, A., D'Amore, L., Hoebenreich, S., Sanchis, J., Lubrano, P., Ferla, M. P., Garcia-Borràs, M., Osuna, S., & Reetz, M. T. (2021). Pervasive cooperative mutational effects on multiple catalytic enzyme traits emerge via long-range conformational dynamics. *Nature Communications*, 12(1), 1621. https://doi.org/10.1038/s41467-021-21833-w.

Arnold, F. H. & Georgiou, G. (2003). *Directed enzyme evolution: Screening and selection methods*. Humana Press. https://stanford.idm.oclc.org/login?url=http://link.springer.com/10.1385/1592593968

Buchan, D. W. A. & Jones, D. T. (2019). The PSIPRED Protein Analysis Workbench: 20 years on. *Nucleic Acids Research*, 47(W1), W402–W407. https://doi.org/10.1093/nar/gkz297.

Chen, Z. & Liu, D. (2016). Toward glycerol biorefinery: Metabolic engineering for the production of biofuels and chemicals from glycerol. *Biotechnology for biofuels*, 9(1), 205. https://doi.org/10.1186/s13068-016-0625-8.

Chiellini, E., Faggioni, S., & Solaro, R. (1990). Polyesters based on glyceric acid derivatives as potential biodegradable materials. *Journal of Bioactive and Compatible Polymers*, 5(1), 16–30. https://doi.org/10.1177/088391159000500103.

Cusa, E., Obradors, N., Baldomà, L., Badía, J., & Aguilar, J. (1999). Genetic analysis of a chromosomal region containing genes required for assimilation of allantoin nitrogen and linked glyoxylate metabolism in Escherichia coli. *Journal of Bacteriology*, 181(24), 7479–7484. https://doi.org/10.1128/jb.181.24.7479-7484.1999.

Datsenko, K. A. & Wanner, B. L. (2000). One-step inactivation of chromosomal genes in *Escherichia coli* K-12 using PCR products. *Proceedings of the National Academy of Sciences*, 97(12), 6640–6645. https://doi.org/10.1073/pnas.120163297.

Demirel, S., Lehnert, K., Lucas, M., & Claus, P. (2007). Use of renewables for the production of chemicals: Glycerol oxidation over carbon supported gold catalysts. *Applied Catalysis B: Environmental*, 70(1-4), 637–643. https://doi.org/10.1016/j.apcatb.2005.11.036.

Dijkman, W. P., de Gonzalo, G., Mattevi, A., & Fraaije, M. W. (2013). Flavoprotein oxidases: Classification and applications. *Applied Microbiology and Biotechnology*, 97(12), 5177–5188. https://doi.org/10.1007/s00253-013-4925-7.

Eriksson, C. P., Saarenmaa, T. P., Bykov, I. L., & Heino, P. U. (2007). Acceleration of ethanol and acetaldehyde oxidation by D-glycerate in rats. *Metabolism*, 56(7), 895–898. https://doi.org/10.1016/j.metabol.2007.01.019.

Forneris, F., Heuts, D. P., Delvecchio, M., Rovida, S., Fraaije, M. W., & Mattevi, A. (2008). Structural analysis of the catalytic mechanism and stereoselectivity in *Streptomyces coelicolor* alditol oxidase. *Biochemistry*, 47(3), 978–985. https://doi.org/10.1021/bi701886t.

Franceus, J., Pinel, D., & Desmet, T. (2017). Glucosylglycerate phosphorylase, an enzyme with novel specificity involved in compatible solute metabolism. *Applied and Environmental Microbiology*, 83(19), e01434–17. https://doi.org/10.1128/aem.01434-17.

Furuyoshi, S., Kawabata, N., Tanaka, H., & Soda, K. (1989). Enzymatic production of D-glycerate from L-tartrate. *Agricultural and Biological Chemistry*, 53(8), 2101–2105. https://doi.org/10.1271/bbb1961.53.2101.

Furuyoshi, S., Nishigouri, J., Kawabata, N., Tanaka, H., & Kenji, S. (1991). D-glycerate production from L-tartrate by cells of *Pseudomonas* sp. with high content of L-tartrate decarboxylase. *Agricultural and Biological Chemistry*, 55(6), 1515–1519. https://doi.org/10.1080/00021369.1991.10870833.

Gerstenbruch, S., Wulf, H., Mußmann, N., O'Connell, T., Maurer, K. H., & Bornscheuer, U. T. (2012). Asymmetric synthesis of D-glyceric acid by an alditol oxidase and directed evolution for enhanced oxidative activity towards glycerol. *Applied Microbiology and Biotechnology*, 96(5), 1243–1252. https://doi.org/10.1007/s00253-012-3885-7.

Gmelch, T. J., Sperl, J. M., & Sieber, V. (2019). Optimization of a reduced enzymatic reaction cascade for the production of L-alanine. *Scientific Reports*, 9(1), 11754. https://doi.org/10.1038/s41598-019-48151-y.

Habe, H., Fukuoka, T., Kitamoto, D., & Sakaki, K. (2009). Biotransformation of glycerol to D-glyceric acid by *Acetobacter tropicalis*. *Applied Microbiology and Biotechnology*, 81(6), 1033–1039. https://doi.org/10.1007/s00253-008-1737-2.

Habe, H., Shimada, Y., Fukuoka, T., Kitamoto, D., Itagaki, M., Watanabe, K., Yanagishita, H., & Sakaki, K. (2009b). Production of glyceric acid by *Gluconobacter* sp. NBRC3259 using raw glycerol. *Bioscience, Biotechnology, and Biochemistry*, 73(8), 1799–1805. https://doi.org/10.1271/bbb.90163.

Habe, H., Shimada, Y., Fukuoka, T., Kitamoto, D., Itagaki, M., Watanabe, K., Yanagishita, H., Yakushi, T., Matsushita, K., & Sakaki, K. (2010). Use of a *Gluconobacter frateurii* mutant to prevent dihydroxyacetone accumulation during glyceric acid production from glycerol. *Bioscience, Biotechnology, and Biochemistry*, 74(11), 2330–2332. https://doi.org/10.1271/bbb.100406.

Habe, H., Shimada, Y., Yakushi, T., Hattori, H., Ano, Y., Fukuoka, T., Kitamoto, D., Itagaki, M., Watanabe, K., Yanagishita, H., Matsushita, K., & Sakaki, K. (2009c). Microbial production of glyceric acid, an organic acid that can be mass produced from glycerol. *Applied and Environmental Microbiology*, 75(24), 7760–7766. https://doi.org/10.1128/AEM.01535-09.

Heo, L., Park, H., & Seok, C. (2013). GalaxyRefine: Protein structure refinement driven by side-chain repacking. *Nucleic Acids Research*, 41(W1), W384–W388. https://doi.org/10.1093/nar/gkt458.

Heuts, D. P., Van Hellemond, E. W., Janssen, D. B., & Fraaije, M. W. (2007). Discovery, characterization, and kinetic analysis of an alditol oxidase from *Streptomyces coelicolor*. *Journal of Biological Chemistry*, 282(28), 20283–20291. https://doi.org/10.1074/jbc.M610849200.

Kumar, M., Madrid, S. M., McDonald, H. C., Poulose, A. J., Rand, T., & Wang, H. (2013a). *Polyol oxidases* (US Patent No. US8383568B2).

Larkin, M. A., Blackshields, G., Brown, N. P., Chenna, R., McGettigan, P. A., McWilliam, H., Valentin, F., Wallace, I. M., Wilm, A., Lopez, R., Thompson, J. D., Gibson, T. J., & Higgins, D. G. (2007). Clustal W and Clustal X version 2.0. *Bioinformatics*, 23(21), 2947–2948. https://doi.org/10.1093/bioinformatics/btm404.

Lešová, K., Šturdíková, M., Proksa, B., Pigoš, M., & Liptaj, T. (2001). OR-1 - a mixture of esters of glyceric acid produced by *Penicillium funiculosum* and its antitrypsin activity. *Folia Microbiologica*, 46(1), 21–23. https://doi.org/10.1007/BF02825878.

Li, Z., Yan, J., Sun, J., Xu, P., Ma, C., & Gao, C. (2018). Production of value-added chemicals from glycerol using in vitro enzymatic cascades. *Communications Chemistry*, 1(1), 71. https://doi.org/10.1038/s42004-018-0070-7.

Martinez, A., Grabar, T. B., Shanmugam, K. T., Yomano, L. P., York, S. W., & Ingram, L. O. (2007). Low salt medium for lactate and ethanol production by recombinant *Escherichia coli* B. *Biotechnology Letters*, 29(3), 397–404. https://doi.org/10.1007/s10529-006-9252-y.

Mattevi, A., Fraaije, M. W., Mozzarelli, A., Olivi, L., Coda, A., & Berkel, W. (1997). Crystal structures and inhibitor binding in the octameric flavoenzyme vanillyl-alcohol oxidase: The shape of the active-site cavity controls substrate specificity. *Structure (London, England)*, 5(7), 907–920. https://doi.org/10.1016/s0969-2126(97)00245-1.

Mukherjee, K., Narindoshvili, T., & Raushel, F. M. (2018). Discovery of a kojibiose phosphorylase in Escherichia coli K-12. *Biochemistry*, 57(19), 2857–2867. https://doi.org/10.1021/acs.biochem.8b00392.

Ness, J. E., Kim, S., Gottman, A., Pak, R., Krebber, A., Borchert, T. V., Govindarajan, S., Mundorff, E. C., & Minshull, J. (2002). Synthetic shuffling expands functional protein diversity by allowing amino acids to recombine independently. *Nature Biotechnology*, 20(12), 1251–1255. https://doi.org/10.1038/nbt754.

Nguyen, Q. T., Romero, E., Dijkman, W. P., de Vasconcellos, S. P., Binda, C., Mattevi, A., & Fraaije, M. W. (2018). Structure-based engineering of *Phanerochaete chrysosporium* alcohol oxidase for enhanced oxidative power toward glycerol. *Biochemistry*, 57(43), 6209–6218. https://doi.org/10.1021/acs.biochem.8b00918.

Ornston, M. K. & Ornston, L. N. (1969). Two forms of D-glycerate kinase in *Escherichia coli*. *Journal of Bacteriology*, 97(3), 1227–1233. https://doi.org/10.1128/jb.97.3.1227-1233.1969.

Peters, B., Mientus, M., Kostner, D., Junker, A., Liebl, W., & Ehrenreich, A. (2013). Characterization of membrane-bound dehydrogenases from *Gluconobacter oxydans* 621H via whole-cell activity assays using multideletion strains. *Applied Microbiology and Biotechnology*, 97(14), 6397–6412. https://doi.org/10.1007/s00253-013-4824-y.

Pettersen, E. F., Goddard, T. D., Huang, C. C., Couch, G. S., Greenblatt, D. M., Meng, E. C., & Ferrin, T. E. (2004). UCSF Chimera–a visualization system for exploratory research and analysis. *Journal of Computational Chemistry*, 25(13), 1605–1612. https://doi.org/10.1002/jcc.20084.

Porta, F. & Prati, L. (2004). Selective oxidation of glycerol to sodium glycerate with gold-on-carbon catalyst: An insight into reaction selectivity. *Journal of Catalysis*, 224(2), 397–403. https://doi.org/10.1016/j.jcat.2004.03.009.

Quan, J. & Tian, J. (2011). Circular polymerase extension cloning for high-throughput cloning of complex and combinatorial DNA libraries. *Nature Protocols*, 6(2), 242–251. https://doi.org/10.1038/nprot.2010.181.

Robert, X. & Gouet, P. (2014). Deciphering key features in protein structures with the new ENDscript server. *Nucleic Acids Research*, 42(W1), W320–W324. https://doi.org/10.1093/nar/gku316.

Roy, A., Kucukural, A., & Zhang, Y. (2010). I-TASSER: A unified platform for automated protein structure and function prediction. *Nature Protocols*, 5(4), 725–738. https://doi.org/10.1038/nprot.2010.5.

Saichana, N., Matsushita, K., Adachi, O., Frébort, I., & Frebortova, J. (2015). Acetic acid bacteria: A group of bacteria with versatile biotechnological applications. *Biotechnology Advances*, 33(6, Part 2), 1260–1271. http://www.sciencedirect.com/science/article/pii/S0734975014001888.

Sato, S., Kitamoto, D., & Habe, H. (2014). *In vitro* evaluation of glyceric acid and its glucosyl derivative, α-glucosylglyceric acid, as cell proliferation inducers and protective solutes. *Bioscience, Biotechnology, and Biochemistry*, 78(7), 1183–1186. https://doi.org/10.1080/09168451.2014.885823.

Sawangwan, T., Goedl, C., & Nidetzky, B. (2009). Single-step enzymatic synthesis of (R)-2-O-α-D-glucopyranosyl glycerate, a compatible solute from micro-organisms that functions as a protein stabiliser. *Organic & Biomolecular Chemistry*, 7(20), 4267–4270. https://doi.org/10.1039/b912621j.

Sun, L. & Yagasaki, M. (2003). Screen for oxidases by detection of hydrogen peroxide with horseradish peroxidase. *Methods in Molecular Biology*, 230, 177–182. https://doi.org/10.1385/1-59259-396-8:177.

Tokuma, F., Shintaro, I., Hiroshi, H., Shun, S., Hideki, S., Masahiko, A., Dai, K., & Keiji, S. (2012). Synthesis and interfacial properties of monoacyl glyceric acids as a new class of green surfactants. *Journal of Oleo Science*, 61(6), 343–348. https://doi.org/10.5650/jos.61.343.

Trott, O. & Olson, A. J. (2010). AutoDock Vina: Improving the speed and accuracy of docking with a new scoring function, efficient optimization, and multithreading. *Journal of Computational Chemistry*, 31(2), 455–461. https://doi.org/10.1002/jcc.21334.

van Hellemond, E. W., Vermote, L., Koolen, W., Sonke, T., Zandvoort, E., Heuts, D. P., Janssen, D. B., & Fraaije, M. W. (2009). Exploring the biocatalytic scope of alditol oxidase from *Streptomyces coelicolor*. *Advanced Synthesis & Catalysis*, 351(10), 1523–1530. https://doi.org/10.1002/adsc.200900176.

Winter, R. T., Heuts, D. P., Rijpkema, E. M., van Bloois, E., Wijma, H. J., & Fraaije, M. W. (2012). Hot or not? Discovery and characterization of a thermostable alditol oxidase from *Acidothermus cellulolyticus* 11B. *Applied Microbiology and Biotechnology*, 95(2), 389–403. https://doi.org/10.1007/s00253-011-3750-0.

Yakushi, T. & Matsushita, K. (2010). Alcohol dehydrogenase of acetic acid bacteria: Structure, mode of action, and applications in biotechnology. *Applied Microbiology and Biotechnology*, 86(5), 1257–1265. https://doi.org/10.1007/s00253-010-2529-z.

Yang, J., Roy, A., & Zhang, Y. (2013). Protein-ligand binding site recognition using complementary binding-specific substructure comparison and sequence profile alignment. *Bioinformatics*, 29(20), 2588–2595. https://doi.org/10.1093/bioinformatics/btt447.

Zelcbuch, L., Razo-Mejia, M., Herz, E., Yahav, S., Antonovsky, N., Kroytoro, H., Milo, R., & Bar-Even, A. (2015). An *in vivo* metabolic approach for deciphering the product specificity of glycerate kinase proves that both *E. coli's* glycerate kinases generate 2-phosphoglycerate. *PLoS One*, 10(3), e0122957. https://doi.org/10.1371/journal.pone.0122957.

Zhan, T., Chen, Q., Zhang, C., Bi, C., & Zhang, X. (2020). Constructing a novel biosynthetic pathway for the production of glycolate from glycerol in *Escherichia coli*. *ACS Synthetic Biology*, 9(9), 2600–2609. https://doi.org/10.1021/acssynbio.0c00404.

Zhan, T., Zhang, K., Chen, Y., Lin, Y., Wu, G., Zhang, L., Yao, P., Shao, Z., & Liu, Z. (2013). Improving glyphosate oxidation activity of glycine oxidase from *Bacillus cereus* by directed evolution. *PLoS One*, 8(11), e79175. https://doi.org/10.1371/journal.pone.0079175.